Development 138, 2069-2078 (2011) doi:10.1242/dev.057745

Polar-localized NPH3-like proteins regulate polarity and endocytosis of PIN-FORMED auxin efflux carriers

Masahiko Furutani[1,*], Norihito Sakamoto[1,*], Shuhei Yoshida[1], Takahito Kajiwara[1], Hélène S. Robert[2,3], Jiří Friml[2,3] and Masao Tasaka[1,†]

SUMMARY

PIN-FORMED (PIN)-dependent auxin transport is essential for plant development and its modulation in response to the environment or endogenous signals. A NON-PHOTOTROPIC HYPOCOTYL 3 (NPH3)-like protein, MACCHI-BOU 4 (MAB4), has been shown to control PIN1 localization during organ formation, but its contribution is limited. The *Arabidopsis* genome contains four genes, *MAB4/ENP/NPY1-LIKE1* (*MEL1*), *MEL2*, *MEL3* and *MEL4*, highly homologous to *MAB4*. Genetic analysis disclosed functional redundancy between *MAB4* and *MEL* genes in regulation of not only organ formation but also of root gravitropism, revealing that NPH3 family proteins have a wider range of functions than previously suspected. Multiple mutants showed severe reduction in PIN abundance and PIN polar localization, leading to defective expression of an auxin responsive marker *DR5rev::GFP*. Pharmacological analyses and fluorescence recovery after photo-bleaching experiments showed that *mel* mutations increase PIN2 internalization from the plasma membrane, but affect neither intracellular PIN2 trafficking nor PIN2 lateral diffusion at the plasma membrane. Notably, all MAB4 subfamily proteins show polar localization at the cell periphery in plants. The MAB4 polarity was almost identical to PIN polarity. Our results suggest that the MAB4 subfamily proteins specifically retain PIN proteins in a polarized manner at the plasma membrane, thus controlling directional auxin transport and plant development.

KEY WORDS: Auxin, PIN, Endocytosis, *Arabidopsis*

INTRODUCTION

The phytohormone auxin is transported from its site of biosynthesis by an intercellular transport system, which is called polar auxin transport. Polar auxin transport establishes asymmetrical auxin distribution in organs and tissues. This process occurs at various developmental stages, such as apical-basal axis formation during embryogenesis, aerial organ formation, root development, vascular patterning, gravitropism, and phototropism (Rolland-Lagen, 2008; Vanneste and Friml, 2009). The auxin efflux carriers of the PIN-FORMED (PIN) family are crucial components of the polar auxin transport (Petrásek et al., 2006). PIN proteins show polar localization at the plasma membrane that correlates with and determines the direction of intercellular auxin flow (Wisniewska et al., 2006).

Several factors that are important for polar PIN delivery have been identified. These include the fact that polar PIN targeting requires a balanced sterol composition in the plasma membrane (Willemsen et al., 2003; Men et al., 2008). In addition, constitutive subcellular dynamics is important for PIN polarity. PIN proteins constitutively undergo clathrin-dependent endocytosis, GNOM-dependent recycling and retromer-dependent vacuolar targeting (Steinmann et al., 1999; Geldner et al., 2003; Jaillais et al., 2006; Dhonukshe et al., 2007; Dhonukshe et al., 2008; Jaillais et al., 2007; Kleine-Vehn et al., 2008). Even though all the mentioned factors influencing PIN polarity, knowledge about the molecular components specifically controlling this process is limited. Phosphorylation of PIN proteins (Zhang et al., 2009; Huang et al., 2010) by a Ser/Thr kinase PINOID (PID) is known to be crucial for apical PIN delivery, while protein phosphatase 2A functions antagonistically (Benjamins et al., 2001; Christensen et al., 2000; Friml et al., 2004; Michniewicz et al., 2007). The *MACCHI-BOU 4/ENHANCER OF PINOID/NAKED PINS IN YUC MUTANTS 1* (*MAB4/ENP/NPY1*) gene was genetically identified as a factor involved in organ formation together with *PID* (Treml et al., 2005; Furutani et al., 2007; Cheng et al., 2007). The gene encodes a NON-PHOTOTROPIC HYPOCOTYL 3 (NPH3)-like protein of unknown function. In cotyledon development, the *mab4* mutation reduces PIN1 abundance in the plasma membrane and when combined with the *pid* mutation it causes complete reversal of PIN1 polarity, indicating that *MAB4* regulates polar auxin transport in organogenesis through the control of PIN1 localization together with *PID*.

In the *Arabidopsis* genome, four genes, *MAB4/ENP/NPY1-LIKE1* (*MEL1*), *MEL2*, *MEL3* and *MEL4* have a noticeably higher level of homology to *MAB4*. Recently, these genes have been reported as *NPY5*, *NPY3*, *NPY4* and *NPY2*, and shown to function redundantly with *MAB4* in organ formation (Cheng et al., 2008). Here, we show, using genetic analysis, the functional redundancy between *MAB4* and *MEL* genes not only in organ formation but also in root gravitropism, thus demonstrating more extensive functions of *MAB4* subfamily genes. In multiple mutants of the *MAB4* subfamily members, the abundance and polar localization of PIN proteins were severely reduced, leading to defective expression of *DR5rev::GFP*, an auxin responsive marker (Friml et al., 2003). Pharmacological analyses showed that *mel* mutations affected PIN2 internalization from the plasma membrane, but did not affect intracellular PIN2 trafficking. Furthermore, all MAB4 subfamily proteins are localized at the cell periphery with polarity

[1]Graduate School of Biological Sciences, Nara Institute of Science and Technology (NAIST), Nara 630-0192, Japan. [2]Department of Plant Systems Biology, Flanders Institute for Biotechnology, B-9052 Gent, Belgium. [3]Department of Plant Biotechnology and Genetics, Ghent University, B-9052 Gent, Belgium.

*These authors contributed equally to this work
†Author for correspondence (m-tasaka@bs.naist.jp)

Accepted 16 February 2011

in plants. The MAB4 polarity was almost identical to PIN polarity. These results suggest that the MAB4 subfamily proteins specifically regulate the retention of PIN proteins in the plasma membrane with polarity in auxin-related morphogenesis.

MATERIALS AND METHODS

Plant materials and growth conditions

Arabidopsis thaliana ecotype Columbia (Col) was used as wild type. The following mutant alleles were used: *mab4-1* (Col), *mab4-2* (Col) (Furutani et al., 2007) and *pin1-201* (Col) (Furutani et al., 2004). *mel1-1* (GABI_027H10), *mel1-2* (SAIL_792_G03), *mel2-1* (SALK_072281), *mel2-2* (SALK_119048), *mel3-1* (SALK_142094), *mel3-2* (SALK_058416), *mel4-1* (SALK_023554) and *mel4-2* (SALK_046452) were obtained from the ABRC (*Arabidopsis* Biological Resource Center) and NASC (Nottingham *Arabidopsis* Stock Centre) (Alonso et al., 2003; Sessions et al., 2002; Rosso et al., 2003) (see Fig. S1 in the supplementary material). *pin2-201* (SAIL_177_A12) carries a T-DNA insertion at the 4th exon and is supposed to be a null allele. This allele was obtained from the Syngenta Arabidopsis Insertion Library (SAIL) and was backcrossed five times to Col prior to root gravitropism assay (Sessions et al., 2002). Plants were grown on soil as previously reported (Fukaki et al., 1996), and siliques were collected for analyses of reporter assay and embryo immunolocalization. For analyses of root gravitropism assay and reporter assay, seeds were surface sterilized and germinated on Murashige and Skoog plates, as previously described (Furutani et al., 2004).

Transgenic plants

To construct the plasmid *promoter* (*pro*)*MEL:MEL-GFP*, *MEL1-4* promoters, the 2.9 kb, 2.9 kb, 2.9 kb and 2.7 kb 5′ sequence of respective genes, were inserted into the binary destination vector *pGWB4*, which contains a Gateway conversion cassette in front of the *GFP*-coding region (*GWB* vectors were kindly provided by Dr Tsuyoshi Nakagawa, Shimane University, Japan) (Nakagawa et al., 2007). Full-length cDNA of *MEL1*, *MEL2*, *MEL3* and *MEL4* were inserted into the *pGWB4* including each promoter. For *35S:MAB4-GFP*, the *MAB4*-coding region was inserted into the *pGWB5* between the cauliflower mosaic virus 35S promoter and the *GFP*-coding region. The resulting plasmids were introduced into *Agrobacterium tumefaciens* strain MP90. *proMEL1:MEL1-GFP*, *proMEL3:MEL3-GFP* and *proMEL4:MEL4-GFP* vectors were transformed into the *mel1-1 mel2-1 mel3-1 mel4-1* quadruple plants by the floral dip method (Clough and Bent, 1998). *proMEL2:MEL2-GFP* was transformed into heterozygous *mab4-2* and homozygous *mel2-1* plants. Transformants were selected on germination medium containing 30 μg/ml kanamycin. Homozygous lines were identified in the T3 generation, and T3 or T4 homozygous lines were used for reporter analysis.

Microscopy

For histological analysis, roots tips were stained with 50 μg/ml of propidium iodide (Sigma-Aldrich), and fluorescence was imaged by confocal laser-scanning microscopy (FV1000; Olympus). For confocal microscopy, dissected embryos were mounted in 7% glucose and root tips were mounted in MS liquid medium [1/2 MS salt mixture, 1% glucose and 0.05% MES (pH 5.8)]. Whole-mount immunofluorescence was performed manually using a protocol described previously (Sauer et al., 2006). Antibodies were diluted as follows: 1:500 for rabbit anti-MAB4, 1:2000 for rabbit anti-PIN2, 1:1000 for mouse anti-GFP (nacalai tesque; used in Fig. 5), 1:500 for rabbit anti-GFP (Molecular Probes; used in Fig. 6 and Fig. S12 in the supplementary material), 1:500 for Alexa488- and Alexa546-conjugated anti-mouse and rabbit secondary antibodies (Invitrogen; used in Fig. 5), and 1:500 and 1:600 for FITC- and CY3-conjugated anti-mouse and anti-rabbit secondary antibodies (Dianova; used in Fig 6 and Fig. S12 in the supplementary material), respectively. Starch granules were visualized as described previously (Willemsen et al., 1998). FRAP analysis was performed as described previously (Grebe et al., 2003; Men et al., 2008).

Drug applications

Drugs were exogenously applied by incubation of 5-day-old seedlings in MS liquid medium supplemented with FM4-64 [15 mM stock in dimethylsulfoxide (DMSO)] (7.5 μM), BFA (10 mM stock in DMSO) (25/50 μM), cycloheximide (CHX) (10 mM stock in ethanol) (50 μM), wortmannin (10 mM stock in DMSO) (15 μM), Tyrphostin A23 (TyrA23) (30 mM stock in DMSO) (15/30/45/60 μM), Tyrphostin A51 (TyrA51) (30 mM stock in DMSO) (45 μM) or 1-naphthalene acetic acid (NAA) (10 mM stock in DMSO) (10 μM). Control treatments contained an equivalent amount of solvent (DMSO or ethanol). For FM4-64 and BFA treatment experiments, seedlings were rinsed twice in MS liquid medium after 1 hour of treatment. For BFA washout experiments, 5-day-old seedlings were treated with 50 μM BFA for 1 hour and then washed with the MS liquid medium for 2 hours. For wortmannin treatment, seedlings were washed twice in the MS liquid medium after 2 hours of treatment. When we performed CHX-pre-treatment (45 minutes) and co-incubation with CHX and BFA or wortmannin, we obtained the same results as those without CHX pre-treatment and co-incubation. For TyrA23 or TyrA51 treatment, plants were pretreated with TyA23 or TyA51 for 30 minutes, followed by co-incubation with BFA (25 μM) and TyA23 or TyA51.

RESULTS

Functional redundancy between *MAB4* subfamily members at various developmental stages

The *Arabidopsis* genome encodes 31 NPH3-like proteins, most of which have not been well characterized (Kimura and Kagawa, 2006). MAB4 is a member of a small subfamily consisting of five proteins of unknown function. We focus on the four family members MEL1-4, which display higher homology to MAB4 than NPH3 or RPT2 (ROOT PHOTOTROPIC RESPONSE 2) (Motchoulski and Liscum, 1999; Sakai et al., 2000) (see Fig. S1A in the supplementary material). *MEL1* (*At4g37590*), *MEL2* (*At5g67440*), *MEL3* (*At2g14820*) and *MEL4* (*At2g23050*) genes have been also recently reported by Cheng et al., who named them *NPY5*, *NPY3*, *NPY2* and *NPY4*, respectively (Cheng et al., 2008). We identified T-DNA insertion alleles, called *mel1-1*, *mel1-2*, *mel2-1*, *mel2-2*, *mel3-1*, *mel3-2*, *mel4-1* and *mel4-2* (see Fig. S1B,C in the supplementary material). However, we could not identify any phenotypes at various developmental stages in each single mutant background, suggesting that *MAB4* subfamily genes might function redundantly. To investigate the role of *MEL* genes, we combined *mel* mutations with the *mab4* mutation. *mab4* single mutants display mild defects in organ formation including cotyledons and floral organs (Furutani et al., 2007). Both *mel1* and *mel2* mutations enhanced the *mab4* mutant phenotypes, as previously reported (Cheng et al., 2008). The *mel1-1* or *mel2-1* mutation caused severe defects in cotyledon and floral organ development in the *mab4-2* background (data not shown). Subsequently, *mab4-2 mel1-1 mel2-1* triple mutants displayed severe pin-like inflorescences (data not shown). These results indicate that *MEL1* and *MEL2* regulate organ formation redundantly with *MAB4*.

Next, we constructed multiple mutants of *mel* mutants. All combinations of double mutants failed to exhibit obvious phenotypes (data not shown). Among all combination of triple mutants, *mel1-1 mel3-1 mel4-1* and *mel2-1 mel3-1 mel4-1* triple mutants displayed mild defects of root gravitropism (data not shown). Furthermore, the *mel1-1 mel2-1 mel3-1 mel4-1* quadruple mutants exhibited severer defects in root gravitropism. The wild-type roots grew in the direction of gravity (Fig. 1A,C), while the quadruple mutant roots lengthened substantially in a random direction, but responded slightly to gravity (Fig. 1B,C). However, the mutant roots had well-organized cell layers and amyroplasts in columella cells, which function as statoliths in root gravitropism,

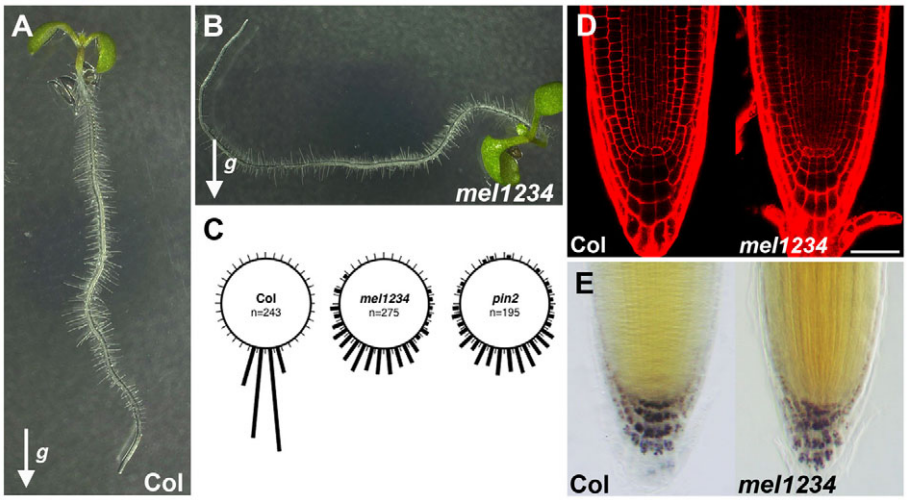

Fig. 1. The function of *MEL* genes in root gravitropism. (**A**,**B**) Five-day-old seedlings of Col (A) and *mel1-1 mel2-1 mel3-1 mel4-1* quadruple mutants (B). Arrows indicate the direction of gravity. (**C**) The growth direction of the primary root in wild-type Col (left), *mel1-1 mel2-1 mel3-1 mel4-1* (middle) and *pin2-201* (right) at 3 days postgermination (dpg). n is the total number of analyzed roots. (**D**) Confocal images of root tip of wild type (left) and *mel1-1 mel2-1 mel3-1 mel4-1* quadruple mutants (right) at 5 dpg. (**E**) Distal root meristem region at 5 dpg of wild-type Col (left) and *mel1-1 mel2-1 mel3-1 mel4-1* quadruple mutants (right). Starch granule staining marks differentiated columella cells (brown). Scale bar: 40 μm.

as seen in wild-type roots (Fig. 1D,E). We also obtained the same results from the other combination of mutant alleles, *mel1-2*, *mel2-2*, *mel3-2* and *mel4-2*, although these quadruple mutants displayed milder defects in root gravitropism than did *mel1-1 mel2-1 mel3-1 mel4-1* (data not shown). These results indicate that *MEL1*, *MEL2*, *MEL3* and *MEL4* gene products mediate the gravity-controlled orientation of the primary root growth redundantly.

Defective PIN localization in *mab4* and *mel* multiple mutants

The phenotypes of *mab4* and *mel* multiple mutants are similar to those of *pin* mutants, namely the pin-like inflorescences in *pin1* mutants and the defective root gravitropism in *pin2* mutants (Fig. 1C) (Okada et al., 1991; Müller et al., 1998; Luschnig et al., 1998). Previously, it was reported that *MAB4/ENP* is important for PIN1 localization during cotyledon development (Treml et al., 2005; Furutani et al., 2007). To test a role for *MAB4* subfamily genes in the control of PIN localization, we analyzed PIN1 localization in cotyledon primordia of *mab4-2 mel1-1 mel2-1* triple mutants, and PIN1 and PIN2 localization in *mel1-1 mel2-1 mel3-1 mel4-1* quadruple mutants. As *mab4-2 mel1-1 mel2-1* triple mutants were sterile, we analyzed PIN1-GFP expression in embryos obtained from siliques of *mab4-2*$^{+/-}$ *mel1-1*$^{-/-}$ *mel2-1*$^{-/-}$ plants. In *mab4-2* embryos, the abundance of PIN1-GFP in the plasma membrane was reduced from the heart stage, as previously reported (Furutani et al., 2007). The reduction of PIN1-GFP expression was restricted to the protodermal cell layer of cotyledon primordia in the *mab4-2* mutant background. By contrast, in embryos of the triple mutants, the severe reduction in the abundance of PIN1-GFP in the plasma membrane was found not only in the protodermal cell layer but also in provascular tissues of cotyledon primordia from the heart stage, although PIN1-GFP was normally expressed in the provasculature of hypocotyle and radicle (Fig. 2A-D). These results indicate that *MEL1* and *MEL2* regulate PIN1 localization in cotyledon development mainly in the provascular tissue in the same way that *MAB4* does in the protodermal cell layer.

Next, we analyzed the localization of PIN1-GFP and PIN2-GFP in agravitropic roots of *mel1-1 mel2-1 mel3-1 mel4-1* quadruple mutants. PIN1-GFP was normally expressed in the stele, pericycle and endodermis of the quadruple roots (Fig. 2E,F). However, PIN1-GFP polarity was disordered in the endodermal cell layer of the quadruple mutants. In the wild type, PIN1-GFP was mainly localized in the basal and inner lateral side of the plasma membrane in endodermal cells (Fig. 2E). Notably, in the mutants, the GFP signal was additionally detectable in the outer lateral side of the plasma membrane (Fig. 2F). To investigate the disruption of PIN1-GFP polarity in more detail, we measured the ratio of GFP intensity at the apical-basal (A-B) side and outer lateral (OL) side of the plasma membrane (see Fig. S2 in the supplementary material). In the *mel1-1 mel2-1 mel3-1 mel4-1* quadruple mutants, the ratio of the A-B density to the OL density was severely lower than that in wild-type roots (Fig. 2N). Next, we analyzed the PIN2-GFP localization in the *mel1-1 mel2-1 mel3-1 mel4-1* roots. In the epidermis and cortex, the abundance of polar localized PIN2-GFP in the plasma membrane was severely reduced, although PIN transcripts were not affected (Fig. 2G; see Fig. S3 in the supplementary material). In addition, we observed an increase in PIN2-GFP signal in the outer lateral side of the plasma membrane in the epidermis of the quadruple mutants compared with wild type (Fig. 2H,I). Subsequently, we measured the ratio of PIN2-GFP intensity between the A-B and OL sides of the plasma membrane in wild type and quadruple mutants. The intensity ratio of A-B side to OL side strongly decreased in the quadruple mutants (Fig. 2O). To investigate whether *mel* mutations specifically affect PIN localization, we analyzed the localization of the non-PIN protein EGFP-LTI6a, which is localized all over the plasma membrane, in wild type and quadruple mutants (Capel et al., 1997; Navarre and Goffeau, 2000; Cutler et al., 2000). We could not detect any differences in EGFP-LTI6a expression between wild type and the quadruple mutants (Fig. 2J-M). When we also calculated the ratio of GFP intensity of the A-B side of the plasma membrane to that of the OL side, there was no difference between them (Fig. 2P). These results indicate that *MEL1*, *MEL2*, *MEL3* and *MEL4* specifically regulate the polarized localization of PIN1 and PIN2 proteins in the root tip.

Auxin response in *mab4* and *mel* multiple mutants

Next, we investigated the distribution of the auxin response in the various combinations of *mab4* and *mel* mutations. To achieve this, we analyzed the expression pattern of the auxin responsive marker, *DR5rev::GFP* in *mab4-2 mel1-1 mel2-1* embryos and *mel1-1 mel2-1 mel3-1 mel4-1* roots. As reported previously (Friml et al., 2003), in heart-stage embryos, *DR5rev::GFP* was expressed in the tips of two cotyledon primordia and radicle (Fig. 3A,B), sometimes the

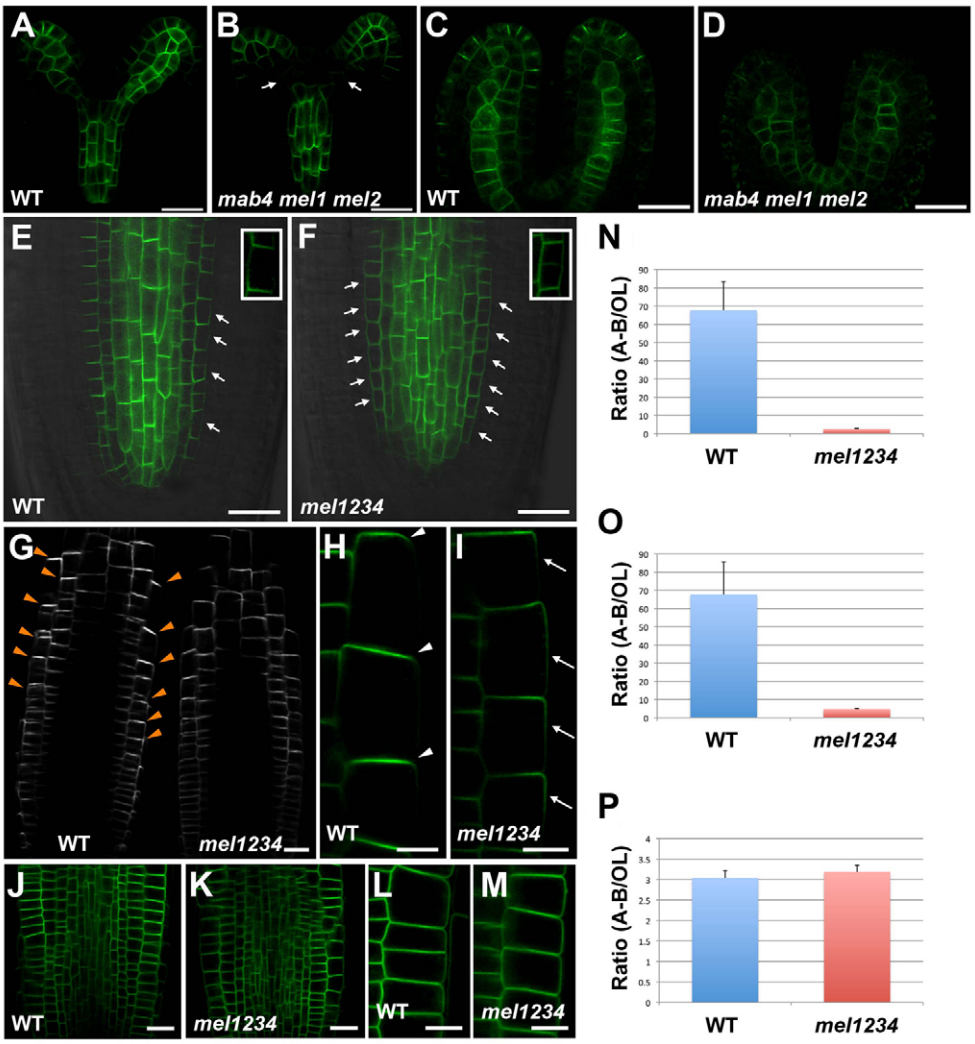

Fig. 2. The *MAB4* subfamily genes regulate PIN localization. (**A-D**) PIN1-GFP expression in wild-type embryos (A,C) and *mab4-2 mel1-1 mel2-1* embryos (B,D) at the heart stage (A,B) and torpedo stage (C,D). Arrows in B indicate the severe reduction of PIN1-GFP expression. (**E**,**F**) PIN1-GFP expression in Col (E) and *mel1-1 mel2-1 mel3-1 mel4-1* (F) roots at 5 dpg. Insets demonstrate magnified images of PIN1-GFP expression in endodermis. (**G**) Confocal image of PIN2-GFP expression in two arranged roots of wild type (left) and *mel1-1 mel2-1 mel3-1 mel4-1* quadruple mutants (right). (**H**,**I**) PIN2-GFP expression in epidermal cells of wild-type (H) and *mel1-1 mel2-1 mel3-1 mel4-1* (I) roots at 5 dpg. (**J-M**) EGFP-LTI6a expression in epidermal cells of wild-type (J,L) and *mel1-1 mel2-1 mel3-1 mel4-1* (K,M) roots at 5 dpg. Right side of images in H,I,L,M is outer side of the root. Arrows in E,F,I indicate the GFP signal on outer lateral (OL) side of the plasma membrane. Arrowheads in G,H demonstrate the polarized PIN2-GFP florescence on the apical side of the plasma membrane. (**N-P**) The ratios of GFP intensity on A-B side to that on OL side of the plasma membrane in wild-type and *mel1-1 mel2-1 mel3-1 mel4-1* roots at 5 dpg. The graph in N displays the ratio of intensity of PIN1-GFP fluorescence on A-B side to that on OL side in the endodermal cells of wild type (blue bar) and *mel1-1 mel2-1 mel3-1 mel4-1* mutants (red bar) [N_{WT}=47 (4 roots), $N_{mel1234}$=73 (4 roots)]. (O) The graph of PIN2-GFP ratio of OL side to A-B side in the epidermal cells of control (blue) and *mel1-1 mel2-1 mel3-1 mel4-1* mutants (red) [N_{WT}=30 (7 roots), $N_{mel1234}$=35 (7 roots)]. (P) The EGFP-LTI6a ratio of A-B side to OL side in the epidermis of wild-type (blue) and *mel1-1 mel2-1 mel3-1 mel4-1* (red) [N_{WT}=33 (6 roots), $N_{mel1234}$=33 (6 roots)]. Error bars represent s.e.m. Scale bars: 20 μm in A-G,J,K; 10 μm in H,I,L,M.

expression was detectable in only one primordium. Later, additional signal of *DR5rev::GFP* was found in the provascular tissues (Fig. 3C,D). By contrast, in the *mab4-2 mel1-1 mel2-1* embryos, expression of *DR5rev::GFP* often disappeared in the apical region of the embryo, although *DR5rev::GFP* was widely expressed in the basal region of the embryo (Fig. 3E,F). At the torpedo stage, the GFP signal in the provascular tissue was restricted to the tops of cotyledon primordia (Fig. 3G,H). We also found an aberrant expression pattern of *DR5rev::GFP* in *mel1 mel2 mel3 mel4* roots. Expansion of *DR5rev::GFP* expression was observed in the lateral root caps, but not in wild-type roots (Fig. 3I,J). These results indicate that the establishment of auxin maxima was disturbed in *mab4-2 mel1-1 mel2-1* embryos and *mel1-1 mel2-1 mel3-1 mel4-1* roots correlating with the disordered polar PIN localization.

Affected PIN2 internalization from the plasma membrane in *mel* multiple mutants

To investigate how *mel* mutations affect polar localization of PIN proteins, we analyzed the lateral mobility of functional PIN2-GFP at the plasma membrane in *mel1 mel2 mel3 mel4* mutants by fluorescence recovery after photo-bleaching (FRAP) experiments.

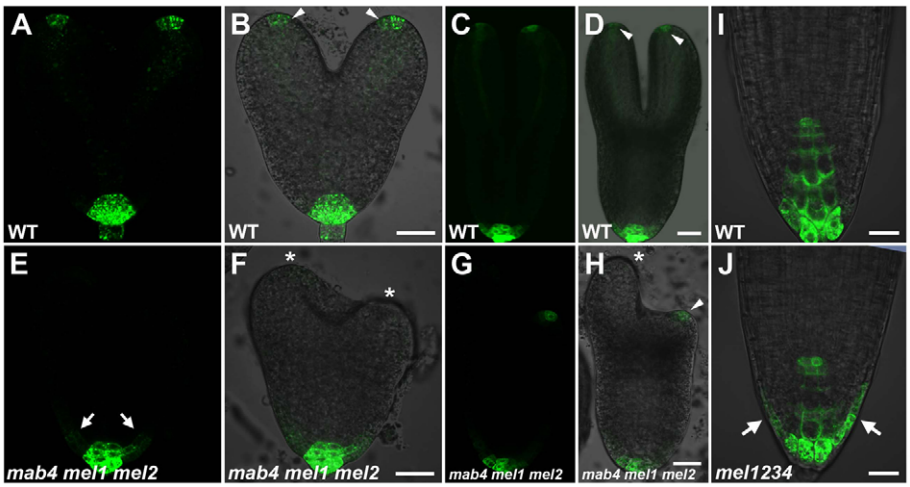

Fig. 3. The *MAB4* subfamily regulates auxin distribution. (**A-D**) *DR5rev::GFP* expression in wild-type embryos at the heart (A,B) and torpedo (C,D) stages. (**E-H**) *DR5rev::GFP* expression in *mab4-2 mel1-1 mel2-1* embryos at the heart (E,F) and torpedo (G,H) stages. (**I**,**J**) *DR5rev::GFP* expression in root tips of wild type (I) and *mel1-1 mel2-1 mel3-1 mel4-1* quadruple mutant (J) at 5 dpg. GFP fluorescence images (A,C,E,G) and merged images with Nomarski images (B,D,F,H,I,J). Arrowheads in B,D,H indicate *DR5rev::GFP* expression in the tips of cotyledon primordia. By contrast, asterisks in F and H represent the disappearance of GFP signal in the protoderm cells of cotyledon primordia. Arrows in E,J show the expanded expression of *DR5rev::GFP* in the tips of radicle and root. Scale bars: 20 μm.

We bleached PIN2-GFP fluorescence from the plasma membrane and monitored FRAP in roots treated with the protein biosynthesis inhibitor CHX and energy inhibitors, which abolish energy-dependent traffic. FRAP kinetics monitoring lateral diffusion did not obviously differ between wild-type and *mel1-1 mel2-1 mel3-1 mel4-1* mutant cells in which fluorescence had been bleached at the plasma membrane (see Fig. S4A-C in the supplementary material). Therefore, our findings show that *mel* mutations do not appear to affect the rate of PIN2-GFP lateral diffusion when membrane trafficking is blocked.

To address another possibility that *mel* mutations affect PIN trafficking, PIN2-GFP trafficking was analyzed in the mutants. PIN proteins continuously undergo endocytosis and recycling between the plasma membrane and endosomes. Furthermore, PIN proteins are sorted to the lytic vacuolar compartments via a pre-vacuolar compartment (PVC). Treatment with the vesicle trafficking inhibitors BFA and wortmannin, affects PIN trafficking at the respective points of drug action. BFA treatment inhibits PIN recycling and leads to PIN accumulation in aggregated endosomes, so called BFA compartments. Wortmannin affects localization of vacuolar sorting receptors and alters the PVC identity, leading to PIN2 relocalization to wortmannin-induced compartments. When *mel1-1 mel2-1 mel3-1 mel4-1* or wild-type roots were treated with BFA or wortmannin, PIN2-GFP was internalized into the BFA compartment or wortmannin-induced compartments (see Fig. S5A,B,E,F in the supplementary material). To investigate the sensitivity to the drug in the quadruple mutants in more detail, we treated roots with a range of BFA concentrations. However, we could not detect any differences in sensitivity between wild type and the quadruple mutants (data not shown). The effects of BFA treatment on vesicle trafficking are reversible. When BFA was washed from the medium, the BFA compartments disappeared and PIN2-GFP reverted to the plasma membrane (see Fig. S5C in the supplementary material). In *mel* quadruple mutants, BFA washout led to reversion to normal recycling of PIN2-GFP to the plasma membrane in a similar manner to wild-type roots (see Fig. S5D in the supplementary material). These results indicate that *mel* mutations do not affect the recycling of PIN2 proteins back to the plasma membrane. Taken together, the results suggest that intracellular trafficking of PIN2-GFP is unaffected in mel multiple mutants. To investigate PIN internalization mediated by clathrin-dependent endocytosis in the mutants, we treated PIN2-GFP expressing plants with TyrA23, an inhibitor of recruitment of endocytic cargo into the clathrin-mediated pathway, in the presence of BFA (Ortiz-Zapater et al., 2006; Dhonukshe et al., 2007). In the wild-type root, only the endocytic tracer FM4-64 accumulated in BFA compartments, whereas PIN2-GFP was retained at the plasma membrane (Fig. 4A). Similar results were also obtained for the plasma membrane protein, EGFP-LTI6a. TyrA23, but not a close structural analog, TyrA51, inhibited the BFA-induced internalization of EGFP-LTI6a (Fig. 4C; see Fig. S6 in the supplementary material). By contrast, in *mel1-1 mel2-1 mel3-1 mel4-1* roots treated with TyrA23 and BFA, PIN2-GFP accumulated in BFA compartments where it colocalized with FM4-64 (Fig. 4B), although EGFP-LTI6a was retained in the plasma membrane (Fig. 4D). To examine the sensitivity to TyrA23, treatment was performed over a wide range of concentrations. TyrA23 blocked PIN2 internalization in a concentration-dependent manner, but the mutants were less sensitive than wild type (see Fig. S7 in the supplementary material). In addition, auxin treatment was recently reported to block PIN internalization from the plasma membrane. We exogenously treated PIN2-GFP-expressing seedlings with auxin in the presence of BFA and examined the effects on PIN internalization in the *mel* multiple mutants. PIN2-GFP was kept in the plasma membrane of wild-type cells, whereas PIN2-GFP accumulated in the intracellular compartments in the mutant cells (Fig. 4E,F). These results indicate that *mel* mutations specifically modulate clathrin-dependent PIN2 internalization from the plasma membrane.

Overlapping, unique expression patterns of polarized MEL proteins

To examine the organ- and tissue-specific expression patterns of the *MAB4* and *MEL* genes in plants, promoter fragments of *MAB4*, *MEL1*, *MEL2*, *MEL3* and *MEL4* were fused to the β-*glucuronidase* (*GUS*) reporter gene and introduced into *Arabidopsis* wild-type plants. Furthermore, we performed in situ hybridization using specific anti-sense probes for each gene. We obtained the same results with regard to expression pattern using these two methods (see Figs S8, S9, S10 in the supplementary material). The signal from *proMAB4:GUS*, *proMEL1:GUS* and *proMEL2:GUS* was detected in organ primordia such as cotyledons, leaves and floral organs (see Figs S8, S10 in the supplementary material). In the radicle and root, the promoter of the *MAB4* and all MEL genes was

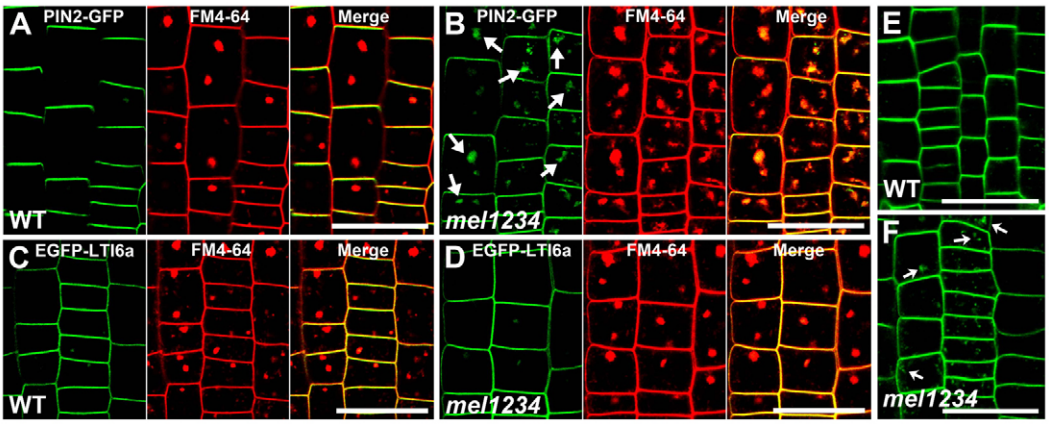

Fig. 4. *mel* mutations affect the internalization of PIN2-GFP. (**A**,**B**) Confocal images of the fluorescence of GFP (green, left), FM4-64 (red, middle) in the epidermal cells of 45 μM TyrA23, BFA-treated seedling expressing PIN2-GFP at 5 dpg of wild type (A) and *mel1-1 mel2-1 mel3-1 mel4-1* (B). Co-labeling with GFP and FM4-64 marks yellow signal (right). Arrows indicate PIN2-GFP localization in BFA compartments. (**C**,**D**) Internalization of EGFP-LTI6a into BFA compartments was inhibited by treatment with TyrA23 in wild type (C) and *mel1-1 mel2-1 mel3-1 mel4-1* (D). (**E**,**F**) Confocal images of the fluorescence of GFP in the epidermal cells of 10 μM NAA, BFA-treated seedling expressing PIN2-GFP at 5 dpg of wild type (E) and *mel1-1 mel2-1 mel3-1 mel4-1* (F). Arrows indicate PIN2-GFP localization in BFA compartments. Scale bars: 30 μm.

strongly active (see Fig. S8 in the supplementary material). Interestingly, we also found activity of the *MEL1* and *MEL2* promoters in stomatal lineage cells of cotyledons and true leaves (see Fig. S8F,I in the supplementary material). These results indicate that the expression patterns of *MAB4*, *MEL1* and *MEL2* mark active proliferating organs, including shoot meristem, young leaf primordia and floral organ primordia, whereas in the root tip *MAB4*, *MEL1*, *MEL2*, *MEL3* and *MEL4* were expressed in an overlapping unique manner. These expression patterns are consistent with the results of genetic analyses.

To investigate the functional domain of MAB4 and MEL proteins in plant cells, we performed immunolocalization analysis for MAB4 using a MAB4-specific antibody and expressed functional MEL-GFP fusion proteins under the control of their own promoters. To confirm the specificity of the MAB4 antibody, we performed immunolocalization analysis towards wild-type and *mab4* embryos, and compared the signal between them. In the wild-type embryos, the signals were detected in the domain where the *MAB4* mRNA is detectable, whereas signals were not detectable in the *mab4* embryos (see Fig. S11 in the supplementary material). The functionality of the corresponding MEL-GFP fusion proteins was confirmed by complementation of the mutant phenotype. In wild-type embryos, MAB4 was localized in the periphery of protodermal cells with polarity at the early heart stage (Fig. 5A). The MAB4 polarity was converged to the tips of cotyledon primordia (Fig. 5A). It has previously been reported that PIN1 polarity was also converged toward the tips of cotyledon primordia in the protodermal cell layer (Benková et al., 2003). To investigate the spatial and temporal relationship between MAB4 and PIN1 localizations during embryogenesis, we performed double-immunostaining analysis using MAB4- and GFP-specific antibodies in the PIN1-GFP-expressing embryos. At the globular and heart stage, MAB4 was colocalized with PIN1-GFP in the protodermal cells (Fig. 5B-D). These results indicate that MAB4 was localized peripherally with polarity in the outer cells, and that MAB4 polarity was absolutely identical to PIN1 polarity. Next, to examine the subcellular localization of MEL proteins, we analyzed the localization of the functional MEL-GFP in the embryo. MEL1-GFP was localized in the upper side of the plasma membrane towards the tips of cotyledon primordia in the protodermal cells, and in the basal side of provascular cells and radicle tip cells (Fig. 5E-G). In the *proMEL2:MEL2-GFP*-expressing plants, MEL2-GFP signals were detected in the identical domains to MEL1-GFP signals (data not shown). MEL3-GFP was basally localized in the plasma membrane in the QC and columella initial cells, and weakly in the cytosol (Fig. 5H-J). MEL4-GFP was basally localized in the provascular cells of the basal region and radicle tips (Fig. 5K-N). Furthermore, we analyzed the localization of MEL proteins in the root expressing functional MEL-GFP proteins. In the stele, pericycle, endodermis and cortex, MEL1-GFP was basally localized, whereas in the epidermis it was in the upper side of the plasma membrane (Fig. 6A,B). In the QC and columella cells, MEL1-GFP was localized weakly in the cytosol, sometimes close to the basal side of the plasma membrane (see Fig. S12A in the supplementary material). The localization pattern of MEL2-GFP and MEL4-GFP was almost identical to that of MEL1-GFP in the root (data not shown; Fig. 6E,F). In the epidermis, the signal of MEL3-GFP was detected in the upper side of the plasma membrane (Fig. 6C,D). In the QC and columella initial cells, MEL3-GFP was weakly localized in the cytosol, sometimes close to the basal side of the plasma membrane (see Fig. S12B in the supplementary material). These results indicate that MEL proteins are mainly localized in the cell periphery with polarity; however, in specific cells such as QC and columella initial cells, MEL proteins tend to diffuse into the cytosol sometimes close to the plasma membrane. In addition, in the domain where expression of MEL genes is overlapping, the subcellular distribution pattern of their proteins was completely identical.

PIN proteins are internalized from the plasma membrane and then recycled to the plasma membrane or targeted to the vacuole through endosomes. To investigate whether polarized MEL proteins are also internalized from the plasma membrane and traffic between the intracellular compartments, we performed a pharmacological analysis using BFA as an inhibitor of vesicle trafficking. Interestingly, when we treated *proMEL1:MEL1-GFP*-expressing plants with BFA, we could not find any change in the

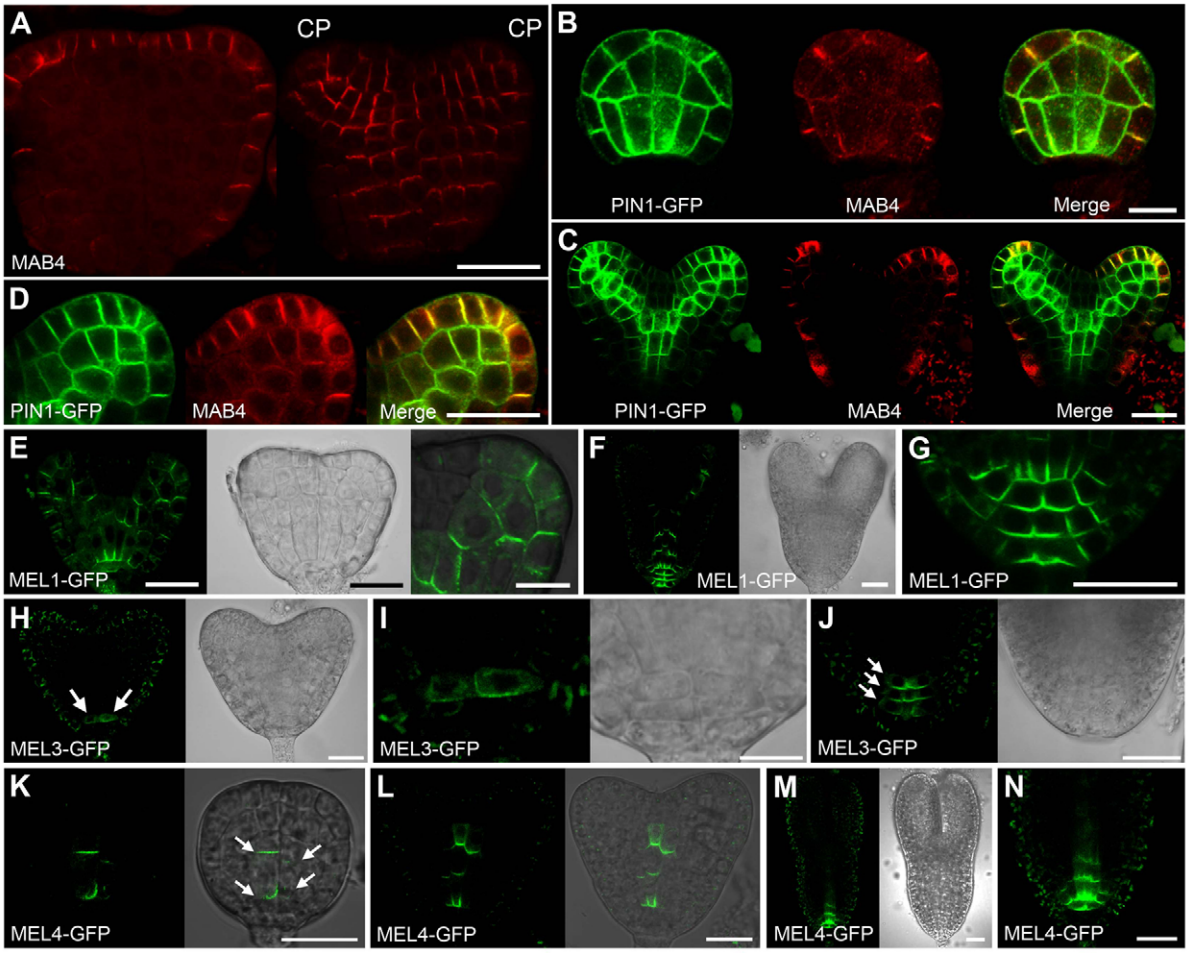

Fig. 5. MAB4 and MEL-GFP localization during embryogenesis. (**A**) MAB4 localization at the early heart stage. CP indicates cotyledon primordium. (**B-D**) Immunolocalization of PIN1-GFP (green) and MAB4 (red) localization at the globular (B) and heart (C,D) stage. (D) A magnified image of cotyledon primordium in C. (**E-G**) MEL1-GFP localization at the transition (E) and heart (F,G) stages. (E) GFP fluorescence image (left), Nomarski image (middle) and merged and magnified image of cotyledon primordium (right). (G) A magnified image of the tip of radicle in F. (**H-J**) MEL3-GFP expression at the early-heart (H,I) and torpedo (J) stage. GFP fluorescence images (left) and Nomarski image (right). The signal in the protodermal cells is autofluorescence of chloroplasts. (**K-N**) MEL4-GFP expression at the globular (K), early-heart (L) and torpedo (M,N) stage. (K,L) GFP fluorescence images (left) and merged images with Nomarski image (right). (M) GFP fluorescence image (left) and Nomarski image (right). (N) A magnified image of the tip of radicle in M. Arrows in H,J,K indicate polarized GFP fluorescence. Scale bars: 20 μm in A,C-N; 10 μm in B.

MEL1-GFP signal close to the plasma membrane, although the fluorescence of FM4-64 presented in the BFA compartments (Fig. 6G-I). Under the same conditions, PIN2-GFP accumulated in the BFA compartments and co-stained with FM4-64 in the epidermis of the root (Fig. 6J-L). In addition, we performed double-immunostaining analysis using PIN2 and GFP specific antibodies in BFA-treated *proMEL3:MEL3-GFP* roots. The GFP signal was localized to the cell periphery, while PIN2 was localized not only in the plasma membrane but also in the BFA compartments (Fig. 6M-P). These results indicate that MEL proteins are not internalized from the plasma membrane and that their localization is confined to the cell periphery, whereas PIN2 proteins are internalized.

Effects of the *pin1* mutation and exogenous auxin treatment on MAB4 localization

To examine whether polar localization of the MAB4 protein depends on the PIN proteins, we analyzed MAB4 localization in embryos developing in *pin1-201*/+ siliques. The mutant embryos were confirmed by cotyledon defects. The abundance of MAB4 in the plasma membrane was significantly reduced in *pin1* embryos (Fig. 7A,B). If the observed effects of the *pin1* mutation on the MAB4 localization were caused by changes in auxin distribution, the exogenous application of auxin could also affect the localization. When *35S:MAB4-GFP* seedlings were treated with synthetic auxin NAA, the signal of MAB4-GFP in the plasma membrane became weak and its polarity was slightly disturbed (Fig. 7C-F). These results indicate that correct auxin distribution, possibly established by PIN proteins, is important in the MAB4 localizations in the plasma membrane.

DISCUSSION

Here, we show functional redundancy between *MAB4* subfamily genes in auxin-related morphogenesis, not only in organ formation but also root gravitropism. In their multiple mutants, PIN abundance in the plasma membrane was severely reduced with weakened polarity. Pharmacological analysis demonstrated that the mutations affected PIN internalization from the plasma membrane,

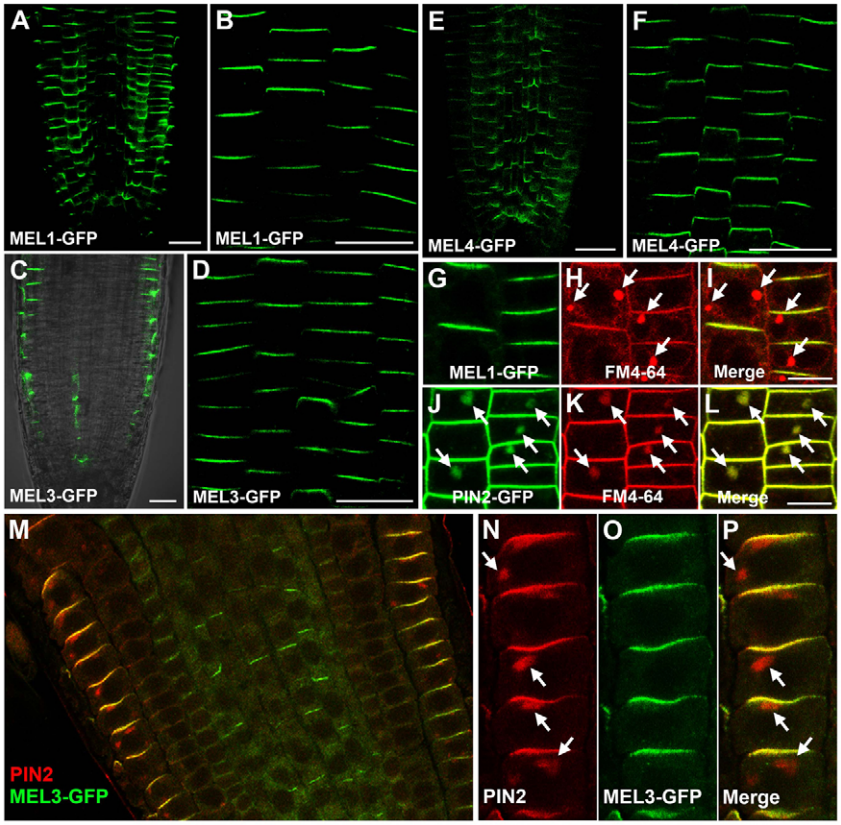

Fig. 6. MEL-GFP localization in root tips. (**A-F**) Localization of MEL1-GFP (A,B), MEL3-GFP (C,D) and MEL4-GFP (E,F) in the root tip at 3 dpg. (B,D,F) MEL1-GFP (B), MEL3-GFP (D) and MEL4-GFP (F) localization in the epidermis. (**G-L**) Confocal images of the fluorescence of GFP (green, G,J), FM4-64 (red, H,K) in the epidermal cells of BFA-treated seedling expressing MEL1-GFP (G,I) and PIN2-GFP (J,L) at 5 dpg. Co-labeling with GFP and FM4-64 marks yellow signal (I,L). (**M-P**) Immunofluorescence in the MEL3-GFP expressing root tip (M) and epidermal cells (N-P) at 3 dpg. PIN2 (red, N) and MEL-3GFP (green, O) were fluorescently double labeled. Arrows indicate BFA compartments. Scale bars: 20 μm.

but did not affect intracellular PIN trafficking. In addition, all MAB4 subfamily proteins are localized at the cell periphery, with polarity almost identical to PIN polarity. Our data suggest that the MAB4 subfamily proteins specifically regulate polarity and endocytosis of PIN proteins in the plasma membrane.

Functional redundancy of *MAB4* subfamily genes in auxin-regulated morphogenesis

MAB4, besides functionally redundant genes *MEL1*/*NPY5* and *MEL2*/*NPY3*, has been identified as a factor that regulates organ formation through the control of polar auxin transport (Furutani et al., 2007; Treml et al., 2005; Cheng et al., 2008). Besides organ formation, our results show a crucial and redundant role for *MEL* genes in root gravitropism. *mel1 mel2 mel3 mel4* quadruple mutants displayed defects in root gravitropism, as did *pin2* mutants and plants treated with an inhibitor of polar auxin transport, indicating that *MEL* genes control polar auxin transport in root gravitropism as well as during organ formation (Fig. 1). In addition, NPH3-like proteins RPT2 and NPH3 have been reported to function in the phototropism of hypocotyl and root, where polar auxin transport is also involved (Motchoulski and Liscum, 1999; Sakai et al., 2000). These data suggest that the *NPH3* family generally might control polar auxin transport in plant development and its modulation in response to the environment or endogenous signals. However, the currently understood functions of *NPH3* family members are not the full story in various aspects of polar auxin transport regulated development. We could not find obvious vascular development phenotypes regulated by polar auxin transport in any combinations of *mel* mutations, even though some *MEL* genes are expressed in vascular tissues. This raises the possibility of additional redundancy at this developmental stage. The genes *At3g26490*, *At1g67900* and *At5g47800* are candidate redundant factors that belong to the subclass that includes the *MAB4* and *MEL* genes. The prospective analyses of these genes and delineation of their relationship to *MAB4* family genes would provide insight into all functions of the *NPH3* family genes.

MAB4 subfamily proteins regulate PIN polarity and internalization in the plasma membrane

MAB4 was reported to control polar auxin transport through the control of PIN1 localization during cotyledon development (Treml et al., 2005; Furutani et al., 2007). Our results show that mutations of the *MEL* genes also specifically affect PIN localization, but not general plasma membrane protein localization (Fig. 2). This is seen in the polar localization of the MAB4 subfamily proteins in the cell periphery, which is almost identical to that of PIN proteins (Figs 5, 6). These observations lead to the suggestion that the *MAB4* subfamily genes specifically control the localization of the corresponding PIN proteins in their expression domains at the various developmental stages.

PIN proteins in the plasma membrane are constitutively internalized to the endosomes as well as to other plasma membrane proteins. Some of them are recycled back to the plasma membrane depending on the activity of GNOM, and others are targeted to the lytic vacuole in a retromer-dependent manner and degraded there. Our pharmacological analysis and FRAP experiment in the mutant background suggest that *mel* mutations affect PIN2 internalization from the plasma membrane, but neither the lateral mobility nor intracellular vesicle trafficking of PIN2 proteins (Fig. 4; see Figs S4, S5 in the supplementary material). In addition, the insensitivity of the MAB4 subfamily proteins to BFA treatment indicates that the functional site is the plasma membrane and not the intracellular

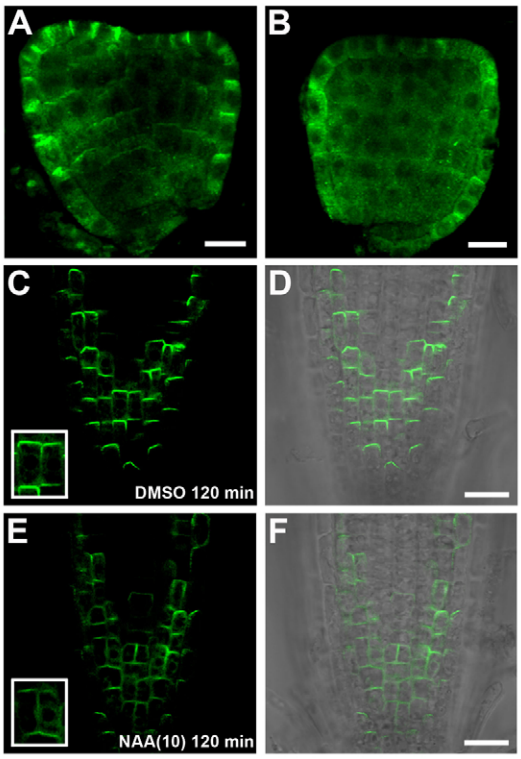

Fig. 7. MAB4 localization in *pin1* embryo and auxin-treated root. (**A**,**B**) MAB4 localization in wild-type-like embryo (A) and *pin1-201* embryo (B) in *pin1-201*/+ siliques. (**C-F**) MAB4-GFP localization in root tips of *35S:MAB4-GFP* seedling treated with DMSO (C,D) and 10 μM NAA (E,F) for 120 minutes. GFP fluorescence images (C,E) and merged images with Nomarski images (D,F). Insets demonstrate magnified images of MAB4-GFP expression in inner cells of root tips. Scale bars: 10 μm in A,B; 20 μm in C-F (13 μm in insets).

compartments (Fig. 6). Taken together, our results suggest that the MAB4 subfamily specifically regulates endocytosis of PIN proteins to maintain its polar localization. This begs the question as to the mechanism of action of the *MAB4* subfamily in retention of PIN localization. It is possible that the MAB4 subfamily blocks the internalization of PIN proteins from the plasma membrane. Mutations of *MAB4* subfamily genes could enhance PIN2 internalization leading to the reduction of polarized PIN2 abundance and lateral relocation by recycling. This scenario is consistent with previous reports that PIN1 internalization from lateral and apical membranes established basal polarity and interference with PIN1 endocytosis prevents PIN1 polarization (Dhonukshe et al., 2008). PIN proteins are retained at the membrane where the MAB4 subfamily proteins are localized, whereas PIN proteins are internalized where the MAB4 subfamily proteins are not. Recently, PID and related AGC kinases were reported to trigger endocytosis-dependent apical PIN recycling through direct phosphorylation of PIN proteins (Michniewicz et al., 2007; Dhonukshe et al., 2010). PID is localized all over the plasma membrane in a non-polarized fashion, whereas MAB4 localization is polarized. These data suggest that PID subfamily promotes PIN internalization in the absence of MAB4 subfamily, while MAB4 subfamily accumulates PIN proteins in the plasma membrane, maybe through the control the activity of PID. Furthermore, a recent study demonstrated that AUXIN-BINDING PROTEIN 1 (ABP1) recruits clathrin to the plasma membrane to promote endocytosis and that auxin binding to ABP1 interferes with this action (Robert et al., 2010). Considering that *mel* mutations affected PIN localization specifically, the MAB4 subfamily might confine the ABP1-mediated signaling to PIN endocytosis.

MAB4 polarity and PIN polarity

In cells displaying PIN polarization in the plasma membrane, the MAB4 subfamily proteins certainly exhibit identical polar localization patterns. However, in specific cells, such as columella and QC cells, the signals from MAB4 family proteins were slightly diffused in the cytosol (see Fig. S12 in the supplementary material), whereas PIN proteins are localized all over the plasma membrane (Friml et al., 2002a; Friml et al., 2002b). This situation is very similar to PIN apolarization in *mel* multiple mutants. It is, thus, conceivable that the MAB4 polarization in the cell periphery strongly correlates with PIN polarity. Cells displaying inconsistency between MAB4 and PIN localization patterns accumulate more auxin than do neighboring cells, as seen by the fact that *DR5rev::GFP* is highly expressed in columella and QC cells. In addition, we show defective PIN localization and auxin distribution in the mutants of the *MAB4* subfamily genes and vice versa (Figs 2, 3, 7). These strongly suggest the existence of a feedback regulation in the establishment of the MAB4 and PIN polarity. Which came first: MAB4 polarity or PIN polarity? At this moment, it is a chicken and egg situation. Further detailed analyses will provide us with insights into the molecular mechanisms that control cell polarity in the polar auxin transport system.

Acknowledgements

We thank Ben Scheres for providing us with PIN1-GFP expressing plants, and ABRC and NASC for providing materials. We also thank Asami Mori for excellent technical assistance. This work was partly supported by a Ministry of Education, Culture, Sports, Science and Technology, through Grant in Aid for Scientific Research on Priority Areas (14036222) to M.T., by Grant-in-Aid for Young Scientists (20770034), and by Global COE Program in NAIST (Frontier Biosciences: strategies for survival and adaptation in a changing global environment), MEXT, Japan to M.F.

Competing interests statement

The authors declare no competing financial interests.

Supplementary material

Supplementary material for this article is available at
http://dev.biologists.org/lookup/suppl/doi:10.1242/dev.057745/-/DC1

References

Alonso, J., Stepanova, A., Leisse, T., Kim, C., Chen, H., Shinn, P., Stevenson, D., Zimmerman, J., Barajas, P., Cheuk, R. et al. (2003). Genome-wide insertional mutagenesis of *Arabidopsis thaliana*. *Science* **301**, 653-657.

Benjamins, R., Quint, A., Weijers, D., Hooykaas, P. and Offringa, R. (2001). The PINOID protein kinase regulates organ development in *Arabidopsis* by enhancing polar auxin transport. *Development* **128**, 4057-4067.

Benková, E., Michniewicz, M., Sauer, M., Teichmann, T., Seifertová, D., Jürgens, G. and Friml, J. (2003). Local, efflux-dependent auxin gradients as a common module for plant organ formation. *Cell* **115**, 591-602.

Capel, J., Jarillo, J., Salinas, J. and Martínez-Zapater, J. (1997). Two homologous low-temperature-inducible genes from Arabidopsis encode highly hydrophobic proteins. *Plant Physiol.* **115**, 569-576.

Cheng, Y., Qin, G., Dai, X. and Zhao, Y. (2007). NPY1, a BTB-NPH3-like protein, plays a critical role in auxin-regulated organogenesis in *Arabidopsis*. *Proc. Natl. Acad. Sci. USA* **104**, 18825-18829.

Cheng, Y., Qin, G., Dai, X. and Zhao, Y. (2008). *NPY* genes and AGC kinases define two key steps in auxin-mediated organogenesis in *Arabidopsis*. *Proc. Natl. Acad. Sci. USA* **105**, 21017-21022.

Christensen, S., Dagenais, N., Chory, J. and Weigel, D. (2000). Regulation of auxin response by the protein kinase PINOID. *Cell* **100**, 469-478.

Clough, S. and Bent, A. (1998). Floral dip: a simplified method for *Agrobacterium*-mediated transformation of *Arabidopsis thaliana*. *Plant J.* **16**, 735-743.

Cutler, S., Ehrhardt, D., Griffitts, J. and Somerville, C. (2000). Random GFP::cDNA fusions enable visualization of subcellular structures in cells of *Arabidopsis* at a high frequency. *Proc. Natl. Acad. Sci. USA* **97**, 3718-3723.
Dhonukshe, P., Aniento, F., Hwang, I., Robinson, D. G., Mravec, J., Stierhof, Y. D. and Friml, J. (2007). Clathrin-mediated constitutive endocytosis of PIN auxin efflux carriers in *Arabidopsis*. *Curr. Biol.* **17**, 520-527.
Dhonukshe, P., Tanaka, H., Goh, T., Ebine, K., Mähönen, A., Prasad, K., Blilou, I., Geldner, N., Xu, J., Uemura, T. et al. (2008). Generation of cell polarity in plants links endocytosis, auxin distribution and cell fate decisions. *Nature* **456**, 962-966.
Dhonukshe, P., Huang, F., Galvan-Ampudia, C. S., Mähönen, A. P., Kleine-Vehn, J., Xu, J., Quint, A., Prasad, K., Friml, J., Scheres, B. et al. (2010). Plasma membrane-bound AGC3 kinases phosphorylate PIN auxin carriers at TPRXS(N/S) motifs to direct apical PIN recycling. *Development* **137**, 3245-3255.
Friml, J., Wiśniewska, J., Benková, E., Mendgen, K. and Palme, K. (2002a). Lateral relocation of auxin efflux regulator PIN3 mediates tropism in *Arabidopsis*. *Nature* **415**, 806-809.
Friml, J., Benková, E., Blilou, I., Wisniewska, J., Hamann, T., Ljung, K., Woody, S., Sandberg, G., Scheres, B., Jürgens, G. et al. (2002b). AtPIN4 mediates sink-driven auxin gradients and root patterning in *Arabidopsis*. *Cell* **108**, 661-673.
Friml, J., Vieten, A., Sauer, M., Weijers, D., Schwarz, H., Hamann, T., Offringa, R. and Jürgens, G. (2003). Efflux-dependent auxin gradients establish the apical-basal axis of *Arabidopsis*. *Nature* **426**, 147-153.
Friml, J., Yang, X., Michniewicz, M., Weijers, D., Quint, A., Tietz, O., Benjamins, R., Ouwerkerk, P., Ljung, K., Sandberg, G. et al. (2004). A PINOID-dependent binary switch in apical-basal PIN polar targeting directs auxin efflux. *Science* **306**, 862-865.
Fukaki, H., Fujisawa, H. and Tasaka, M. (1996). Gravitropic response of inflorescence stems in *Arabidopsis thaliana*. *Plant Physiol.* **110**, 933-943.
Furutani, M., Vernoux, T., Traas, J., Kato, T., Tasaka, M. and Aida, M. (2004). *PIN-FORMED1* and *PINOID* regulate boundary formation and cotyledon development in *Arabidopsis* embryogenesis. *Development* **131**, 5021-5030.
Furutani, M., Kajiwara, T., Kato, T., Treml, B., Stockum, C., Torres-Ruiz, R. and Tasaka, M. (2007). The gene *MACCHI-BOU 4/ENHANCER OF PINOID* encodes a NPH3-like protein and reveals similarities between organogenesis and phototropism at the molecular level. *Development* **134**, 3849-3859.
Geldner, N., Anders, N., Wolters, H., Keicher, J., Kornberger, W., Muller, P., Delbarre, A., Ueda, T., Nakano, A. and Jürgens, G. (2003). The *Arabidopsis* GNOM ARF-GEF mediates endosomal recycling, auxin transport, and auxin-dependent plant growth. *Cell* **112**, 219-230.
Grebe, M., Mobius, W., Ueda, T., Nakano, A., Geuze, H. J., Rook, M. B. and Scheres, B. (2003). *Arabidopsis* sterol endocytosis involves actin-mediated trafficking via ARA6-positive early endosome. *Curr. Biol.* **13**, 1378-1387.
Huang, F., Zago, M. K., Abas, L., van Marion, A., Galván-Ampudia, C. S. and Offringa, R. (2010). Phosphorylation of conserved PIN motifs directs *Arabidopsis* PIN1 polarity and auxin transport. *Plant Cell* **22**, 1129-1142.
Jaillais, Y., Fobis-Loisy, I., Miège, C., Rollin, C. and Gaude, T. (2006). AtSNX1 defines an endosome for auxin-carrier trafficking in *Arabidopsis*. *Nature* **443**, 106-109.
Jaillais, Y., Santambrogio, M., Rozier, F., Fobis-Loisy, I., Miège, C. and Gaude, T. (2007). The retromer protein VPS29 links cell polarity and organ initiation in plants. *Cell* **130**, 1057-1070.
Kimura, M. and Kagawa, T. (2006). Phototropin and light-signaling in phototropism. *Curr. Opin. Plant Biol.* **9**, 503-508.
Kleine-Vehn, J., Leitner, J., Zwiewka, M., Sauer, M., Abas, L., Luschnig, C. and Friml, J. (2008). Differential degradation of PIN2 auxin efflux carrier by retromer-dependent vacuolar targeting. *Proc. Natl. Acad. Sci. USA* **105**, 17812-17817.
Luschnig, C., Gaxiola, R., Grisafi, P. and Fink, G. (1998). EIR1, a root-specific protein involved in auxin transport, is required for gravitropism in *Arabidopsis thaliana*. *Genes Dev.* **12**, 2175-2187.
Men, S., Boutté, Y., Ikeda, Y., Li, X., Palme, K., Stierhof, Y., Hartmann, M., Moritz, T. and Grebe, M. (2008). Sterol-dependent endocytosis mediates post-cytokinetic acquisition of PIN2 auxin efflux carrier polarity. *Nat. Cell Biol.* **10**, 237-244.
Michniewicz, M., Zago, M., Abas, L., Weijers, D., Schweighofer, A., Meskiene, I., Heisler, M., Ohno, C., Zhang, J., Huang, F. et al. (2007). Antagonistic regulation of PIN phosphorylation by PP2A and PINOID directs auxin flux. *Cell* **130**, 1044-1056.
Motchoulski, A. and Liscum, E. (1999). *Arabidopsis* NPH3: a NPH1 photoreceptor-interacting protein essential for phototropism. *Science* **286**, 961-964.
Müller, A., Guan, C., Gälweiler, L., Tänzler, P., Huijser, P., Marchant, A., Parry, G., Bennett, M., Wisman, E. and Palme, K. (1998). *AtPIN2* defines a locus of *Arabidopsis* for root gravitropism control. *EMBO J.* **17**, 6903-6911.
Nakagawa, T., Kurose, T., Hino, T., Tanaka, K., Kawamukai, M., Niwa, Y., Toyooka, K., Matsuoka, K., Jinbo, T. and Kimura, T. (2007). Development of series of gateway binary vectors, pGWBs, for realizing efficient construction of fusion genes for plant transformation. *J. Biosci. Bioeng.* **104**, 34-41.
Navarre, C. and Goffeau, A. (2000). Membrane hyperpolarization and salt sensitivity induced by deletion of *PMP3*, a highly conserved small protein of yeast plasma membrane. *EMBO J.* **19**, 2515-2524.
Okada, K., Ueda, J., Komaki, M. K., Bell, C. J. and Shimura, Y. (1991). Requirement of the auxin polar transport system in early stages of Arabidopsis floral bud formation. *Plant Cell* **3**, 677-684.
Ortiz-Zapater, E., Soriano-Ortega, E., Marcote, M. J., Ortiz-Masiá, D. and Aniento, F. (2006). Trafficking of the human transferrin receptor in plant cells: effects of tyrphostin A23 and brefeldin A. *Plant J.* **48**, 757-770.
Petrásek, J., Mravec, J., Bouchard, R., Blakeslee, J., Abas, M., Seifertová, D., Wisniewska, J., Tadele, Z., Kubes, M., Covanová, M. et al. (2006). PIN proteins perform a rate-limiting function in cellular auxin efflux. *Science* **312**, 914-918.
Robert, S., Kleine-Vehn, J., Barbez, E., Sauer, M., Paciorek, T., Baster, P., Vanneste, S., Zhang, J., Simon, S., C˘ovanová, M. et al. (2010). ABP1 mediates auxin inhibition of clathlin-dependent endocytosis in *Arabidopsis*. *Cell* **143**, 111-121.
Rolland-Lagan, A. (2008). Vein patterning in growing leaves: axes and polarities. *Curr. Opin. Genet. Dev.* **18**, 348-353.
Rosso, M., Li, Y., Strizhov, N., Reiss, B., Dekker, K. and Weisshaar, B. (2003). An *Arabidopsis thaliana* T-DNA mutagenized population (GABI-Kat) for flanking sequence tag-based reverse genetics. *Plant Mol. Biol.* **53**, 247-259.
Sakai, T., Wada, T., Ishiguro, S. and Okada, K. (2000). RPT2. A signal transducer of the phototropic response in Arabidopsis. *Plant Cell* **12**, 225-236.
Sauer, M., Paciorek, T., Benková, E. and Friml, J. (2006). Immunocytochemical techniques for whole-mount in situ protein localization in plants. *Nat. Protoc.* **1**, 98-103.
Sessions, A., Burke, E., Presting, G., Aux, G., McElver, J., Patton, D., Dietrich, B., Ho, P., Bacwaden, J., Ko, C. et al. (2002). A high-throughput Arabidopsis reverse genetics system. *Plant Cell* **14**, 2985-2994.
Steinmann, T., Geldner, N., Grebe, M., Mangold, S., Jackson, C., Paris, S., Gälweiler, L., Palme, K. and Jürgens, G. (1999). Coordinated polar localization of auxin efflux carrier PIN1 by GNOM ARF GEF. *Science* **286**, 316-318.
Treml, B., Winderl, S., Radykewicz, R., Herz, M., Schweizer, G., Hutzler, P., Glawischnig, E. and Ruiz, R. (2005). The gene *ENHANCER OF PINOID* controls cotyledon development in the *Arabidopsis* embryo. *Development* **132**, 4063-4074.
Vanneste, S. and Friml, J. (2009). Auxin: a trigger for change in plant development. *Cell* **136**, 1005-1016.
Willemsen, V., Wolkenfelt, H., de Vrieze, G., Weisbeek, P. and Scheres, B. (1998). The *HOBBIT* gene is required for formation of the root meristem in the *Arabidopsis* embryo. *Development* **125**, 521-531.
Willemsen, V., Friml, J., Grebe, M., van den Toorn, A., Palme, K. and Scheres, B. (2003). Cell polarity and PIN protein positioning in Arabidopsis require *STEROL METHYLTRANSFERASE1* function. *Plant Cell* **15**, 612-625.
Wisniewska, J., Xu, J., Seifertová, D., Brewer, P. B., Ruzicka, K., Blilou, I., Rouquié, D., Benková, E., Scheres, B. and Friml, J. (2006). Polar PIN localization directs auxin flow in plants. *Science* **312**, 883.
Zhang, J., Nodzynski, T., Pencík, A., Rolcík, J. and Friml, J. (2009). PIN phosphorylation is sufficient to mediate PIN polarity and direct auxin transport. *Proc. Natl. Acad. Sci. USA* **107**, 918-922.

Table S1. A list of primer sets for RT-PCR analysis

Gene	Primer set
MEL1	5′-cggaaatggtctcgagcttt-3′ and 5′-ttgatatcttctgtgtccca-3′
MEL2	5′-cttggatccaaacctgattc-3′ and 5′-catctcgagatactcagcag-3′
MEL3	5′-ctgaggatctcaaacttgtt-3′ and 5′-tgattgtcttatgcttcacc-3′
MEL4	5′-gattgtgcatagatctcttc-3′ and 5′-cagtagaagcaatagagccg-3′
PIN1	5′-gcttcatgttactgttcgtcg-3′ and 5′-gatctcttccgtttccgtct-3′
PIN2	5′-gctacacgtggtggttcgaag-3′ and 5′-gactccacttgctccactcg-3′
PIN3	5′-ccaacgcttcacgtcgttcg-3′ and 5′-ggtgacccgtttgagctcca-3′
PIN4	5′-gcttcatgttaccgtgagga-3′ and 5′-gaccggagaagcgcttgagc-3′
PIN7	5′-tcaaacgcttctcggagatc-3′ and 5′-acttgaagaccagctcggtc-3′
ACT8	5′-atgaagattaaggtcgtggca-3′ and 5′-tccgagtttgaagaggctac-3′